

# Modeling Method of CNC Machine Tools' Volume Error Considering Abbe Error

**GUOHUA CHEN**

Hubei University of Arts and Science

**Lin Zhang** (✉ [zjll123456@126.com](mailto:zjll123456@126.com))

Hubei University of Arts and Science <https://orcid.org/0000-0001-8196-5610>

**XIANGJIE WANG**

Hubei University of Arts and Science

**CHAO WANG**

Hubei University of Arts and Science

**HUA XIANG**

Hubei University of Arts and Science

**GUANGQING TONG**

Hubei University of Arts and Science

**DIANZHANG ZHAO**

Hubei University of Arts and Science

---

## Research Article

**Keywords:** Machine tools, Traditional error model, Abbe principle, Body diagonal error, Simulation

**Posted Date:** July 6th, 2021

**DOI:** <https://doi.org/10.21203/rs.3.rs-631290/v1>

**License:**  This work is licensed under a Creative Commons Attribution 4.0 International License.

[Read Full License](#)

---

# Modeling Method of CNC Machine Tools' Volume Error Considering Abbe Error

GUOHUA CHEN<sup>1,2</sup>, LIN ZHANG<sup>1</sup>, XIANGJIE WANG<sup>3</sup>, CHAO WANG<sup>2</sup>, HUA XIANG<sup>2</sup>,  
GUANGQING TONG<sup>2</sup>, DIANZHANG ZHAO<sup>2</sup>

<sup>1</sup>School of Mechanical Engineering, Hubei University of Arts and Science, Xiangyang 441053, China

<sup>2</sup>Institute of Advanced Manufacturing Engineering of Huazhong University of Science and Technology, Xiangyang 441053, China

<sup>3</sup>Mechanical and Electrical Engineering College, Hubei Polytechnic University, Hubei Huangshi 435003, China

Corresponding author: LIN ZHANG (2367742223@qq.com).

**Abstract:** Abbe error is an important factor affecting high-precision machine tools, and the traditional modeling method does not consider Abbe error. Aiming at this problem, based on the traditional error model of machine tools and the formation mechanism of Abbe error, this paper establishes a machine tool spatial error model that considers Abbe error. Then combined with a specific machine tool, based on the measurement of 21 geometric errors of the machine tool to obtain relevant error data, through the combination of qualitative and quantitative accuracy evaluation methods, two models of traditional error model and error model considering Abbe error are analyzed. The accuracy of the machine tool is compared, and the comparison of the compensation effects of the two error models after compensation is also analyzed. The example verification shows that the machine tool spatial error model considering Abbe error is effective and feasible, and the compensation effect is better. It provides an important modeling method for improving the machining accuracy of precision machine tools.

Key words: Machine tools; Traditional error model; Abbe principle; Body diagonal error; Simulation

## 0 introduction

With the continuous developments in science and technology, higher requirements are placed on the machining accuracy of mechanical products<sup>[1,2]</sup>. As widely used equipment in the manufacturing industry, CNC machine tools are facing new challenges and opportunities in the current age.

The measurement of machine tool error is a key step in the improvement of machine tool accuracy and determines the effect of error compensation. There are many classic methods for measuring machine tool errors. Such as a laser tracker<sup>[3-5]</sup>, laser displacement sensor<sup>[6]</sup>, touch-trigger probe<sup>[7,8]</sup>, non-contact optical components<sup>[9]</sup>, R-test device<sup>[10]</sup>, ball plate<sup>[11,12]</sup>. Among the many volume error modeling methods, due to the advantages of simple understanding and wide application range, the homogeneous

coordinate transformation matrix method based on multi-body system theory<sup>[13-15]</sup>, referred to as HTM method, is widely used in three-axis machine tools, five-axis machine tools and In the derivation of the volume error compensation model for multi-axis machining or measuring equipment such as coordinate measuring machines<sup>[16]</sup>. Kim et al. established volume error compensation models for three coordinate measuring machines and three-axis machine tools based on the theory of rigid body kinematics<sup>[17]</sup>. In 2017, Chen and others have attempted to establish a total of 12 polynomial error models for the three-axis linkage of the machine tools based on the error measurement data of the entire working volume of the machine tools, and initially discussed the error prediction methods of the machine tools at different volume positions<sup>[18]</sup>. In 2019, Zuo and others have proposed a method to change the trajectory of the cue working space, and based on this method, carried out volume error modeling, which can accurately solve the rotation error elements of the tool coordinate system and the workbench coordinate system<sup>[19]</sup>. In 2019, Zhang Yueming has established the error-free motion equations between adjacent bodies employing the multi-body theory. Using the adjacent body kinematics theory, he has established the topological structure relationship of each moving part and the low-order body array, and completed the error modeling of the machine tools grinding system, and realized the prediction of the machining accuracy of the machine tools<sup>[20]</sup>. The current measurement and modeling methods for machine tool errors have greatly promoted the improvement of machine tool error compensation technology, but the above-mentioned documents do not consider the positional relationship between the measurement point and the actual processing point. When the center line of the motion axis is inconsistent with the moving direction of the working point of the measuring system, Abbe deviation will occur<sup>[21-24]</sup>, and the main cause of the error source is the deflection error will be amplified by the Abbe deviation. That is, the Abbe error caused by the Abbe deviation will seriously restrict the improvement of the compensation effect of the CNC machine tool.

Based on the analysis of Abbe principle, this paper proposes a machine tool spatial error model that considers Abbe error. By comparing the error data obtained by traditional measurement methods with the error data considering Abbe error, the influence of Abbe error on linear error is analyzed and developed Error compensation module. Finally, an example is verified on the machine tool, and the compensation effect of the traditional error model and the spatial error model of the machine tool considering the Abbe error is analyzed and compared through the quantitative evaluation of the diagonal line and the qualitative evaluation of the matlab simulation.

## **1 Modeling method**

As a traditional modeling method, the homogeneous coordinate transformation method has been widely used in the spatial error modeling of machine tools<sup>[25-27]</sup>. The use of homogeneous coordinate

transformation to derive a comprehensive mathematical model of machine tool error first needs to establish a Cartesian coordinate system on the tool, worktable, spindle, and workpiece. Then, according to the principle of homogeneous coordinate transformation, the description of the dynamic characteristics of each movement pair error and the chain conversion between each movement pair are carried out, and the coordinate conversion matrix between each coordinate system is established. Finally, according to the situation that the tool tip and the cutting point are located at the same point in space, the relationship between the tool coordinate system and the workpiece coordinate system is established, and the equation is solved to obtain a comprehensive mathematical model containing various errors.

$$\begin{aligned}
\Delta x &= -\delta_{xm}(x) - \delta_{xm}(y) + \delta_{xm}(z) - y\varepsilon_{zm}(x) - z\varepsilon_{ym}(x) - z\varepsilon_{ym}(y) + y\alpha_{xy} - z\alpha_{xz} \\
\Delta y &= -\delta_{ym}(x) - \delta_{ym}(y) + \delta_{ym}(z) + z\varepsilon_{xm}(x) + z\varepsilon_{xm}(y) - z\alpha_{yz} \\
\Delta z &= -\delta_{zm}(x) - \delta_{zm}(y) + \delta_{zm}(z) + y\varepsilon_{xm}(x)
\end{aligned} \tag{1}$$

In the formula,  $\Delta x$ ,  $\Delta y$  and  $\Delta z$  represent the position error of the actual cutting point of the tool relative to the ideal cutting point. Furthermore,  $\delta_{xm}(x)$ ,  $\delta_{ym}(x)$ , and  $\delta_{zm}(x)$  are the moving errors in the X direction.  $\varepsilon_{xm}(x)$ ,  $\varepsilon_{ym}(x)$ , and  $\varepsilon_{zm}(x)$  are the angle errors generated when the work bench is moved along the X-axis in the X, Y and Z-directions, respectively.  $\alpha_{xy}$ ,  $\alpha_{xz}$  and  $\alpha_{yz}$  represent the verticality error of the X- to Y-axis, X- to Z-axis and Y- to Z-axis.

## 2 Optimizing the comprehensive error model based on Abbe principle

To establish the machine tool error model it accurately is the key to Perform error compensation. What the laser interferometer measures the error of the machine tool is the movement error of the laser head on the worktable, not the tool tip point error. At the same time, due to the Abbe error, there is a certain difference between the measuring point and the tool tip point error. So, it is more reasonable to consider the comprehensive error modeling of the Traditional error model of Abbe error.

### 2.1 Measurement error conversion

Traditional error model modeling is derived from the kinematics of the mechanism. When using the Traditional error model error compensation model to perform comprehensive error compensation on the machine tool, it is necessary to ensure that the cutting point of the machine tool coincides with the coordinate origin of the workpiece coordinate system and the tool coordinate system. But when using the laser interferometer to measure the geometric error of the machine tool, the position of the tool cutting point is not coincide with the error measuring point in the space. The offset between the two points is shown in Figure 1.

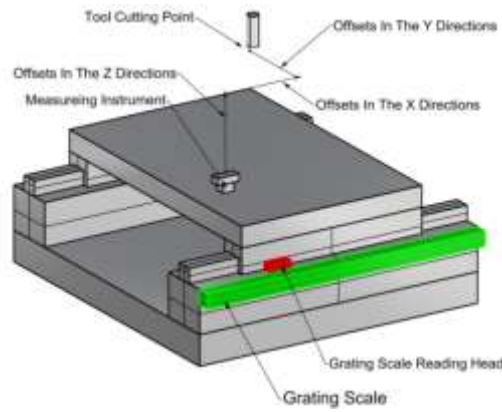


Figure 1 Error measurement point and tool cutting point deviation

On a machine tool with a grating ruler as the position control unit, the position of the motion axis is obtained by real-time feedback of the grating ruler. During processing, the cutting point of the tool and the grating ruler are not on the same axis. There is an Abbe offset in space and an angular error in the machining process. So Abbe error will be introduced at the cutting point of the tool. The true position error of the cutting point of the tool is composed of the positioning error and angle error at the grating ruler and the Abbe error caused by the Abbe deviation.

Assuming that the offset between the cutting point of the tool and the X-axis grating ruler in the Z direction is  $L_z(x)$ , the pitch angle error of the X-axis during movement is  $\varepsilon_{ym}(x)$ , so the Abbe error in the X direction caused by the X-axis pitch angle error at the cutting point of the tool is:  $\varepsilon_{ym}(x) \times L_z(x)$  which is shown in the Figure 2.

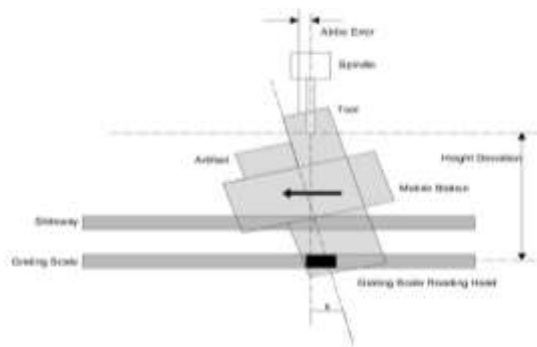


Figure 2 Abbe deviation introduces Abbe error

In actual processing, the cutting point of the tool and the reading head of the grating scale are offset in three directions in space. As shown in Figure 3, the yaw angle error of the motion axis will also introduce Abbe error at the cutting point of the tool. Therefore, the geometric error in the X direction introduced by the X axis at the cutting point of the tool should be composed of three parts: the reference positioning error at the grating ruler, the Abbe error introduced by the pitch angle error, and the Abbe

error introduced by the yaw angle error. The calculation formula is:

$$\delta_{xm}(x) = \delta_{x\alpha}(x) + \varepsilon_{ym}(x)L_z(x) - \varepsilon_{zm}(x)L_y(x) \quad (2)$$

Among them:  $\delta_{x\alpha}$  represents the reference positioning error at the X-axis grating scale reading head,  $\delta_{xm}(x)$  represents the positioning error measured when the measuring axis is the X-axis.  $L_z(x)$  and  $L_y(x)$  is respectively the offsets in the Z and Y directions between the X-axis grating scale reading head and the cutting point of the tool.

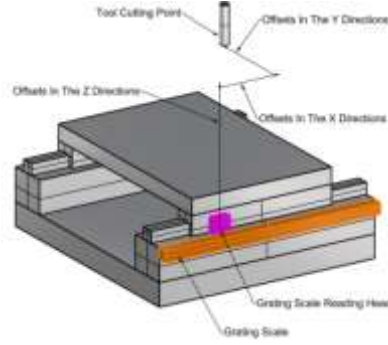


Figure 3 Offset between the cutting point of the tool and the reading head of grating

## 2.2 Error model optimization

It can be seen from the analysis that although the positioning errors obtained from different measurement positions are different, the reference positioning errors at the reading head of the grating ruler contained are all the same. The positioning error measured by the above formula instrument is converted into the reference positioning error at the reading head of the grating ruler and substituted into the compensation model.

When deriving the error model based on the multi-system theory, the six geometric errors of the motion axis must be located at the same position. So when converting the positioning error, it should base on the Bryan principle to convert the straightness error from the measuring point to the grating scale reading head. Since the motion axis can be regarded as a rigid body, the angle error does not need to be converted. The conversion formula of X axis positioning error and straightness error is as follows:

$$\begin{aligned} \delta_{xm}(x) &= \delta_{x\alpha}(x) + \varepsilon_{ym}(x)L_z(x) - \varepsilon_{zm}(x)L_y(x) \\ \delta_{ym}(x) &= \delta_{y\alpha}(x) - \varepsilon_{xm}(x)L_z(x) + \varepsilon_{zm}(x)L_x(x) \\ \delta_{zm}(x) &= \delta_{z\alpha}(x) + \varepsilon_{xm}(x)L_y(x) - \varepsilon_{ym}(x)L_x(x) \end{aligned} \quad (3)$$

Among them:,  $\delta_{x\alpha}$ ,  $\delta_{y\alpha}$  and  $\delta_{z\alpha}$  respectively represent the error value of x, y, z direction at the reading head of the grating ruler.

In the same way, the conversion formula of Y-axis, Z-axis positioning error and straightness error

can be obtained.

And the optimized XYTZ type machine tool comprehensive error model is:

$$\begin{aligned}
 E_x &= -\delta_{x\alpha}(x) - \delta_{x\alpha}(y) + \delta_{x\alpha}(z) - y\varepsilon_{zm}(x) - z\varepsilon_{ym}(x) - z\varepsilon_{ym}(y) + y\alpha_{xy} - z\alpha_{xz} \\
 E_y &= -\delta_{y\alpha}(x) - \delta_{y\alpha}(y) + \delta_{y\alpha}(z) + z\varepsilon_{xm}(x) + z\varepsilon_{xm}(y) - z\alpha_{yz} \\
 E_z &= -\delta_{z\alpha}(x) - \delta_{z\alpha}(y) + \delta_{z\alpha}(z) + y\varepsilon_{xm}(x)
 \end{aligned} \tag{4}$$

### 3 Application verification

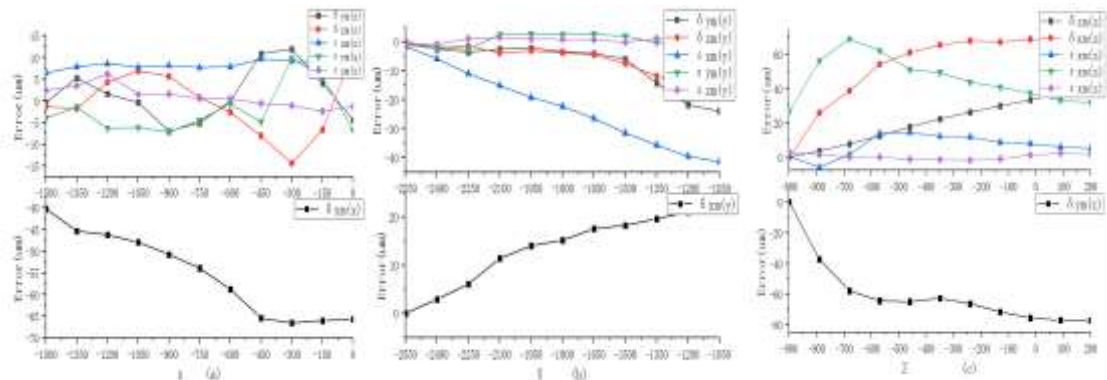
The research object of this paper is the XHK714 three-axis vertical machining center produced by Hubei Jiangshan huake digital equipment technology co., LTD. The characteristic dimensions of the overall structure of the machining center are: 1800mm travel in the X axis direction, 1500mm travel in the Y axis direction, 1200mm travel in the Z axis direction.

#### 3.1.1 Machine errors' data collection

In the case of non-collision and considering the rationality of the experiment, the travel of three axes is selected as follows: X-axis: 0~1500, Y-axis: -2550~-1050, z-axis: -900~200. In the case of meeting the relevant measurement requirements of the country, the measurement spacing is selected to be 150mm, 150mm, 110mm, and the X, Y, and Z axes are all divided into 11 segments. Six geometric errors of X, Y and Z axis were measured with laser interferometer successively, the measurement site is shown in Figure 4. The measurement results are shown in Figure. 4.



Figure 4. measurement site



(a) (b) (c)

Figure 5. Machine tool error measurement data

As shown in Figure. 5(a), the measuring travel of X axis is [0,-1500]mm, and the measuring distance is 150mm. The positioning error is between  $-40.2\mu\text{m}\sim 65.6\mu\text{m}$ . The straightness error is between  $-14.4\mu\text{m}\sim 11.9\mu\text{m}$ , and the angle error is between  $-7.1\mu\text{m}\sim 9.7\mu\text{m}$ .

As shown in Figure. 5(b), the Y-axis measurement stroke is [-2550,-1050]mm, and the measurement interval is 150mm. The positioning error is between  $-0.2\mu\text{m}\sim -24.1\mu\text{m}$ . The straightness error is between  $-18.5\mu\text{m}\sim 22.5\mu\text{m}$ . The angle error is  $-41.4\mu\text{m}\sim 2.7\mu\text{m}$ .

As shown in Figure. 5(c), the Z-axis measurement stroke is [-900,200]mm. The measurement interval is 110mm. The positioning error is between  $0.2\mu\text{m}\sim 41.7\mu\text{m}$ . The straightness error is between  $-77.2\mu\text{m}\sim 68.8\mu\text{m}$ . The angle error is  $-5.7\mu\text{m}\sim 68.9\mu\text{m}$ .

### 3.1.2 Analysis of machine tool geometric error data considering Abbe error

Since the 21-item geometric error data measurement process of the machine tool uses a laser interferometer, the axis of the displacement sensor installed in the laser interferometer is not on the extension line of the motion axis of the measuring head, resulting in an Abbe error, According to formula 10, the linear error data of the machine tool considering the Abbe error are:

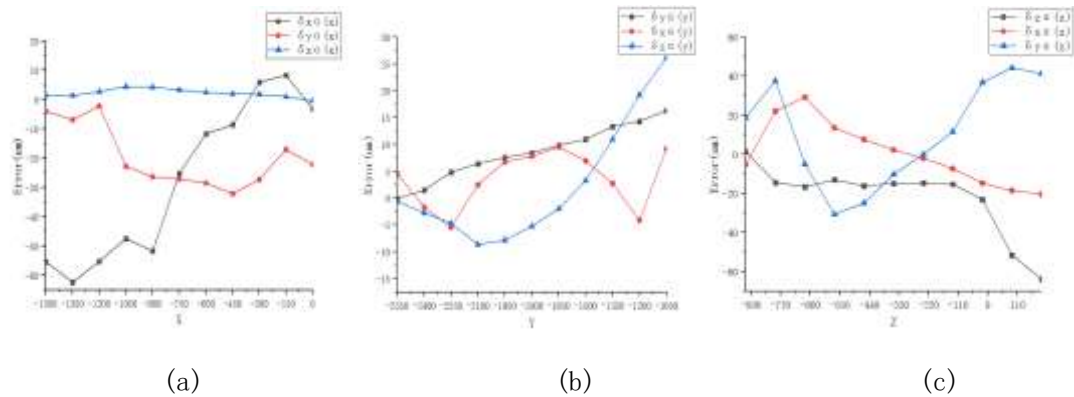


Figure 6. X, Y, Z axis linear error

As shown in Figure.6, the positioning error of X axis is between  $-62.4\mu\text{m}\sim 8.3\mu\text{m}$ . The straightness error is between  $-32.1\mu\text{m}\sim 4.5\mu\text{m}$ . The positioning error of Y axis is between  $-0.1\mu\text{m}\sim 16.3\mu\text{m}$ . The straightness error is between  $-8.7\mu\text{m}\sim 26.1\mu\text{m}$ . The positioning error of Z axis is between  $-63.8\mu\text{m}\sim 1.4\mu\text{m}$ . The straightness error is between  $-30.8\mu\text{m}\sim 44.2\mu\text{m}$ .

Through the comparative analysis of the machine tool error measurement data and the linear error data considering the Abbe error, it is found that due to the existence of the Abbe arm and the influence

of the angle error, the linear error considering the Abbe error is significantly different from the laser interferometer measurement error data. Therefore, it is more accurate to use the traditional error model optimized based on Abbe error.

### 3.2 Simulation evaluation

By linearly fitting the error data measured by the laser interferometer, the 18-item geometric error data model is obtained, and the error data is substituted into formula 1, and the comprehensive error model of the machine tool based on Traditional error model is obtained. By using the MATLAB simulation method, the machine tool comprehensive error model is imported into the error calculation program for calculation, and the volume error ( $\Delta x$ ,  $\Delta y$ ,  $\Delta z$ ) of the characteristic points in the volume error field is obtained. Using matlab simulation tool to perform error interval color separation on the volume error ( $\Delta x$ ,  $\Delta y$ ,  $\Delta z$ ), and we obtain the color separation diagram of the error field as shown in Figure 7.

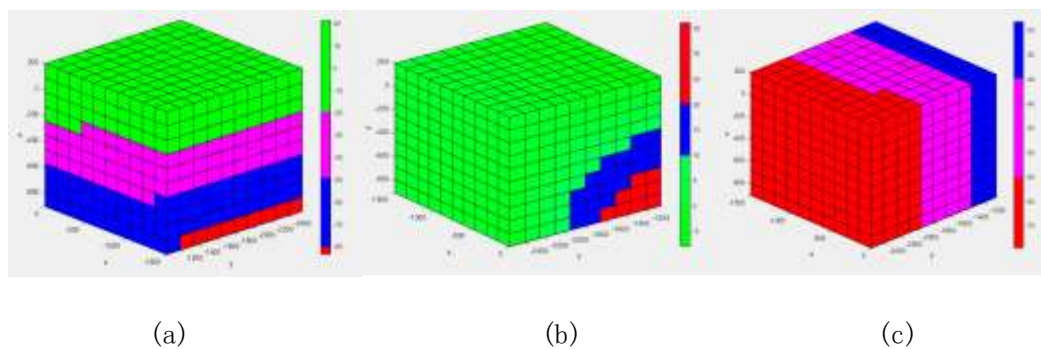


Figure 7. Simulation of XYZ three-dimensional volume error field before compensation. The column (a) represents the simulation of X-direction error field. The column (b) represents the simulation of Y-direction error field. The last column (c) represents the simulation of Z-direction error field.

Figure. 7. (a) reflects the x-direction error  $E_x$  of the machine tools in the whole space. The volume error of X (-1500~0) mm, Y (-2550~-1050) mm, Z (-130~200) mm is within  $20\mu\text{m}$ . The volume error of X (-1350~-1500) mm, Y (-2550~-1200) mm, Z (-900~-790) m has reached  $80\mu\text{m}$ .

Figure. 7. (b) reflects the machine tools Y-direction error  $E_y$  in the entire space. The volume error of X (-1500~0) mm, Y (-2550~-1050) mm, Z (-900~200) mm is within  $10\mu\text{m}$ . One of the few volume errors is between  $10\mu\text{m}$ ~ $35\mu\text{m}$ . The volume error of X (-1500~0) mm, Y (-1650~-1050) mm, Z (-900~-680) m exceeds  $20\mu\text{m}$ .

Figure. 7. (c) reflects the machine tools Z-direction error  $E_z$  in the entire space. The volume error of X (-1500~0) mm, y (-1350~-1050) mm, z (-900~200) mm is within  $40\mu\text{m}$ . The volume error of X (-1500~0) mm, Y (-2550~-1950) mm, Z (-900~200) mm volume exceeds  $60\mu\text{m}$ .

Based on measurement data considering Abbe error through linear fitting, the optimized functions are substituted into formula (4), and the  $x$ ,  $y$ ,  $z$ 's machine tool comprehensive error model is obtained. Use the optimized machine tool space error model, calculate the error data ( $E_x$ ,  $E_y$ ,  $E_z$ ) of each space point of the machine, and use the color separation chart to indicate the error interval range.

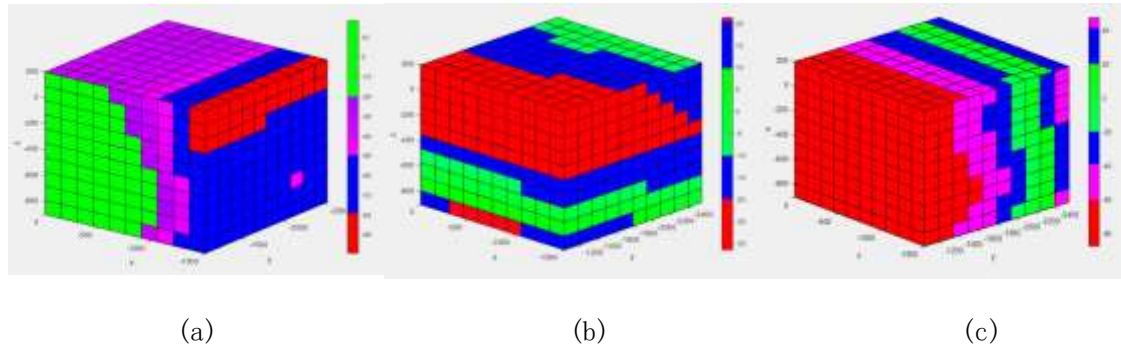


Figure 8. Simulation of XYZ three-term spatial error field after optimization of Abbe error before compensation. The column (a) represents the simulation of X-direction error field. The column (b) represents the simulation of Y-direction error field. The last column (c) represents the simulation of Z-direction error field.

Figure 8. (a) reflects the  $x$ -direction error  $E_x$  of the machine tools in the whole space. The volume error of  $X$  (-1350~1500) mm,  $Y$  (-2550~1050) mm,  $Z$  (-130~200) m has reached  $90\mu\text{m}$ .

Figure 8. (b) reflects the machine tools  $Y$ -direction error  $E_y$  in the entire space. The volume error of  $X$  (-1500~0) mm,  $Y$  (-1050~1500) mm,  $Z$  (-350~200) m exceeds  $20\mu\text{m}$ .

Figure 8. (c) reflects the machine tools  $Z$ -direction error  $E_z$  in the entire space. The volume error of  $X$  (-1500~0) mm,  $Y$  (-1500~1050) mm,  $Z$  (-900~200) mm volume exceeds  $60\mu\text{m}$ .

By analyzing Figures 7 and 8, it can be seen that in the spatial error diagram obtained by the traditional error model simulation, the maximum error in the  $X$  direction is about  $80\mu\text{m}$ , the maximum error in the  $Y$  direction is about  $35\mu\text{m}$ , and the maximum error in the  $Z$  direction is about  $70\mu\text{m}$ . In the spatial error map obtained by the traditional error model simulation based on Abbe error optimization, the maximum error in the  $X$  direction exceeds  $90\mu\text{m}$ , the error in the  $Y$  direction exceeds  $30\mu\text{m}$ , and the maximum error in the  $Z$  direction exceeds  $80\mu\text{m}$ . This shows that the Abbe error has a greater impact on the machine tool space error. From the space error cloud chart, it can be seen that in most of the machine tool space, the space error obtained by simulation based on the traditional error model optimized by the Abbe error is larger than the traditional error model.

### 3.3 Error compensation

#### 3.3.1 Development of compensation system software

After obtaining the compensation data of the execution end of the machine tools, Based on the machine tools volume error model and measured data characteristics, this paper developed a machine tools volume error compensation module on the Huazhong 8 CNC system platform. This module contains basic X, Y and Z axis measurement intervals, grid spacing and grid point settings and compensation file reading functions, and adds volume error compensation parameter settings in the setting parameters, including compensation ratio, compensation switch, etc. . The interface of the compensation module is shown in Figure. 9.

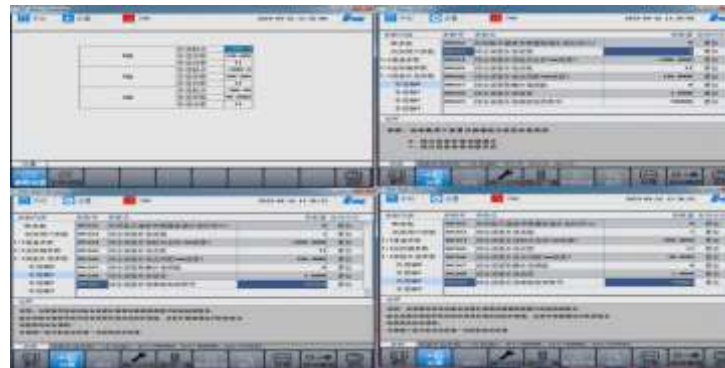


Figure 9. Compensation module interface

### 3.3.2 Precision Evaluation after Compensation

#### 3.3.2.1 Simulation qualitative evaluation

After the system compensation software compensates the machine tool space error based on the Traditional error model error model, the compensation effect is simulated qualitatively evaluated. The machine tool space error field is shown in the Figure 10.

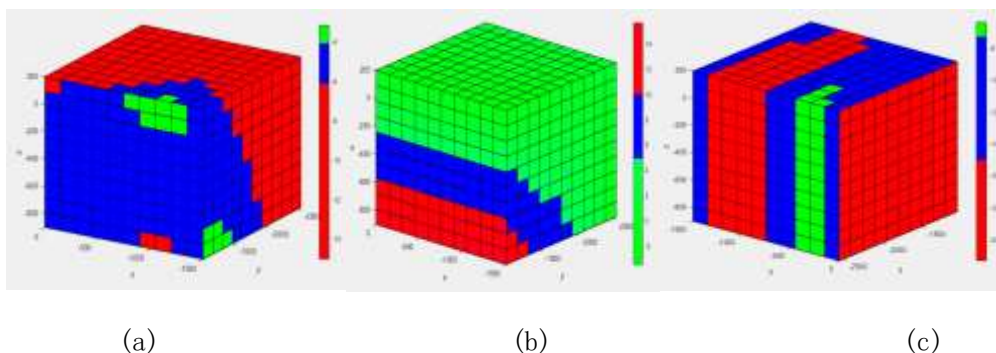


Figure 10. Simulation of XYZ three-dimensional space error field after traditional error compensation model compensation. The column (a) represents the simulation of X-direction error field. The column (b) represents the simulation of Y-direction error field. The last column (c) represents the simulation of Z-direction error field.

Figure. 10. (a) reflects the x-direction error  $E_x$  of the machine tools in the whole space. The volume error of X (0~-1500) mm, Y (-2550~-1950) mm, Z (-900~200) m is between  $6\mu\text{m}$ ~ $14\mu\text{m}$ .

Figure 10. (b) reflects the machine tools Y-direction error  $E_y$  in the entire space. The volume error of X (-1500~0) mm, Y (-2550~-1050) mm, Z (-240~200) m is between  $0\mu\text{m}\sim 5\mu\text{m}$ .

Figure 10. (c) reflects the machine tools Z-direction error  $E_z$  in the entire space. The volume error of X (-750~0) mm, Y (-2550~-1050) mm, Z (-900~200) mm is between  $7\mu\text{m}\sim 15\mu\text{m}$ . One of the few volume errors is within  $7\mu\text{m}$ .

The system compensation software performs spatial error compensation on the Traditional error model comprehensive model considering the optimization of Abbe error, and performs simulation and quantitative evaluation of the compensated machine tool space error. The machine tool space error field is shown in the Figure 11.

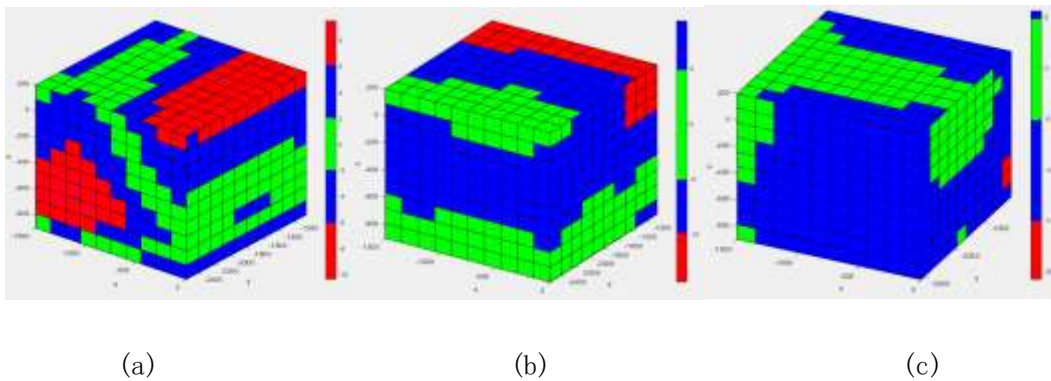


Figure 11. Compensation model based on Abbe error optimization and XYZ three-dimensional spatial error field simulation after compensation. The column (a) represents the simulation of X-direction error field. The column (b) represents the simulation of Y-direction error field. The last column (c) represents the simulation of Z-direction error field.

Figure 11. (a) reflects the x-direction error  $E_x$  of the machine tools in the whole space. The volume error of X (-1500~0) mm, Y (-2550~-1500) mm, Z (-570~90) m is within  $10\mu\text{m}$ .

Figure 11. (b) reflects the machine tools Y-direction error  $E_y$  in the entire space. The volume error of X (-1500~0) mm, Y (-1050~-1500) mm, Z (-350~200) m is between  $5\mu\text{m}\sim 10\mu\text{m}$ .

Figure 11. (c) reflects the machine tools Z-direction error  $E_z$  in the entire space. The volume error of X (-1500~0) mm, Y (-1200~-1050) mm, Z (-790~-570) mm volume exceeds  $15\mu\text{m}$ .

### 3.3.2.2 Quantitative Evaluation of Body Diagonal

At present, the evaluation of the spatial accuracy of machine tools is usually based on the diagonal precision index. In a three-axis CNC machine tool space, there are four body diagonals, the body diagonals can reflect the overall spatial accuracy of the machine tool. In general, the accuracy of the machine tool can only be indicated when the diagonal accuracy indexes of the four bodies are simultaneously high. At present, there is no international standard for body diagonal accuracy. Our

team's previous research showed that the accuracy index of four body diagonal accuracy of a CNC machine tool can be controlled within 20 $\mu$ m at the same time, and the accuracy of the machine tool is very high. In order to evaluate the spatial accuracy of the machine tool, the laser doppler measuring instrument and the step diagonal measuring mirror group are used to measure the whole travel space of the machine tool. The measurement travel plan is shown in Figure 12.

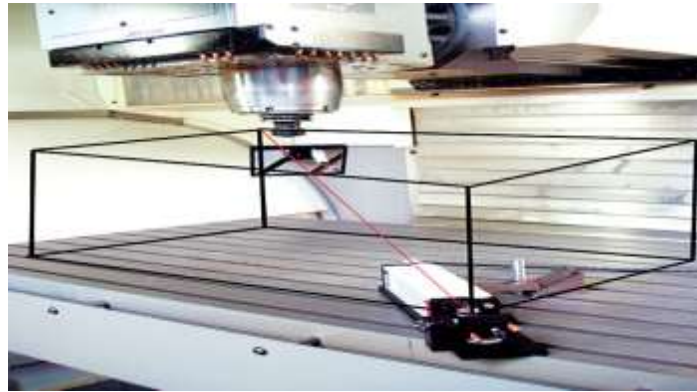


Figure 12. Body diagonal error measurement

The size of the working space of the machine tool for measuring the diagonal of the laser step by step body is 1500 $\times$ 1500 $\times$ 1100mm, divided into  $n=11$  grids. X, Y and Z are measured step by step in each lattice, and the corresponding moving vectors of each step are (150,0,0), (0,150,0) and (0,0,110). The traditional error model, the measurement result of the volume diagonal error is shown in the Figure.

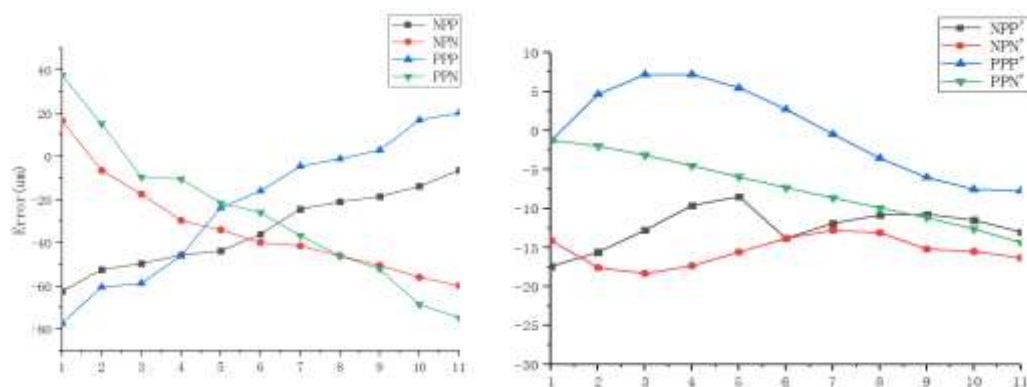


Figure 13. Diagonal error of traditional error model. NPP、NPN、PPP and PPN represents the compensation for the diagonal errors before compensation. NPP'、NPN'、PPP' and PPN' represents the body diagonal errors after compensation

Before compensation, the maximum positioning error of PPP body diagonal is -77.2  $\mu$  m. The maximum positioning error of NPP body diagonal is -62.5  $\mu$  m. The maximum positioning error of PPN body diagonal is -74.6  $\mu$  m, and the maximum positioning error of NPN body diagonal is -66.7  $\mu$  m.

After compensation, the maximum positioning error of PPP' body diagonal is -7.7  $\mu$  m. The

maximum positioning error of NPP' body diagonal is  $-17.4 \mu\text{m}$ . The maximum positioning error of PPN' body diagonal is  $-14.3 \mu\text{m}$ , and the maximum positioning error of NPN' body diagonal is  $-18.7 \mu\text{m}$ .

The compensation system uses a Traditional error model error model optimized based on Abbe error to compensate the machine tool's spatial error, and uses a laser interferometer to measure the machine's diagonal error and quantitatively evaluate the machine's spatial error. The measurement results are shown in Figure 14.

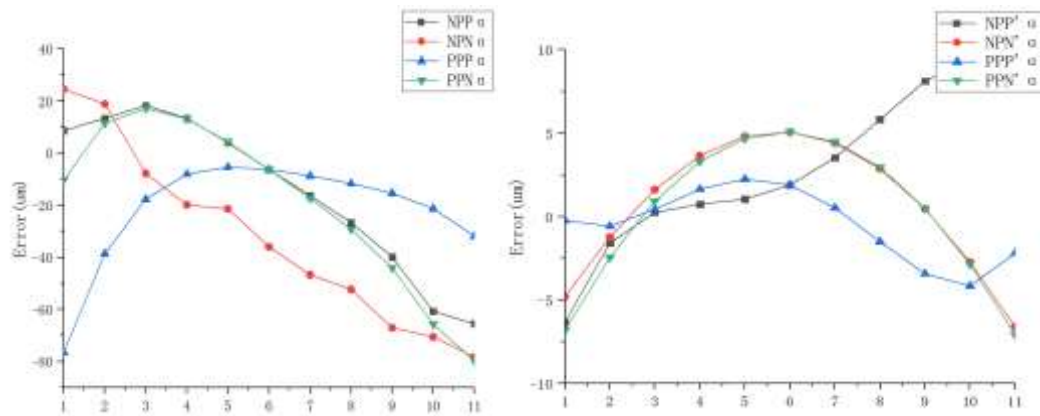


Figure 14. Diagonal error of Traditional error model optimized based on Abbe error. NPP $\alpha$ 、NPN $\alpha$ 、PPP $\alpha$  and PPN $\alpha$  represents the compensation for the diagonal errors before compensation. NPP' $\alpha$ 、NPN' $\alpha$ 、PPP' $\alpha$  and PPN' $\alpha$  represents the body diagonal errors after compensation

Before compensation, the maximum positioning error of PPP $\alpha$  body diagonal is  $-76.5 \mu\text{m}$ . The maximum positioning error of NPP $\alpha$  body diagonal is  $-65.5 \mu\text{m}$ . The maximum positioning error of PPN $\alpha$  body diagonal is  $-79.7 \mu\text{m}$ , and the maximum positioning error of NPN $\alpha$  body diagonal is  $-78.3 \mu\text{m}$ . After compensation, the maximum positioning error of PPP' $\alpha$  body diagonal is  $-4.2 \mu\text{m}$ . The maximum positioning error of NPP' $\alpha$  body diagonal is  $9.4 \mu\text{m}$ . The maximum positioning error of PPN' $\alpha$  body diagonal is  $-7.1 \mu\text{m}$ , and the maximum positioning error of NPN' $\alpha$  body diagonal is  $-6.6 \mu\text{m}$ .

The Abbe error is a factor that is not considered in the traditional error model, but it affects the linear error measurement data, and then affects the accuracy of the traditional error model, and finally has an impact on the compensation effect based on the traditional error model. The specific effects are shown in Table 1.

Table 1 Comparison table of error compensation data before and after Abbe error optimization

			Before compensation(um)	After compensation(um)
Traditional error model	X, Y, Z axis linear error (max)	$\delta m(x)$	65.6	-15.3
		$\delta m(y)$	24.1	-12.8
		$\delta m(z)$	-77.2	-19.2
	Body diagonal error(max)	NPP	-62.5	-17.4
		NPN	-66.7	-18.7
		PPP	-77.2	-7.7
		PPN	-74.6	-14.3
Traditional error model optimized based on Abbe error	X, Y, Z axis linear error(max)	$\delta \alpha(x)$	-62.4	-16.7
		$\delta \alpha(y)$	26.1	-14.2
		$\delta \alpha(z)$	-63.8	-16.5
	Body diagonal error(max)	NPP $\alpha$	-65.5	9.4
		NPN $\alpha$	-78.3	-6.6
		PPP $\alpha$	-76.5	-4.2
		PPN $\alpha$	-79.7	-7.1

In terms of linearity errors, the maximum linear errors of each axis of the traditional error measurement data are 65.6  $\mu$  m, 24.1  $\mu$  m, and -77.2  $\mu$  m respectively, and the actual maximum linear errors of each axis considering the Abbe error are -62.4  $\mu$  m, 26.1  $\mu$  m, and -63.8  $\mu$  m respectively.

In terms of machine tool body diagonal error: Before error compensation, the maximum body diagonal error in the traditional error measurement data is -77.2  $\mu$  m, and the actual maximum body diagonal error data considering the Abbe error is -79.7  $\mu$  m. After error compensation, the maximum volume diagonal error in the traditional error measurement data is -18.7  $\mu$  m, and the actual maximum volume diagonal error data considering the Abbe error is 9.4  $\mu$  m.

Through the comparison and analysis of the specific error data, it can be seen that the Abbe error has a greater impact on the linear error, which in turn has an impact on the compensation effect. Compared with the traditional model, the traditional error model considering the Abbe error has a better compensation effect, and the maximum error of the body diagonal is reduced by 9.3  $\mu$  m.

## 4 Conclusion

At present, traditional error modeling methods do not consider the influence of Abbe error on the measurement results of linear error data. In order to overcome the above shortcomings, based on the influence of the Abbe arm and the angle error on the linear error data measurement result, a machine tool spatial error model considering the Abbe error was established. Secondly, according to the model, a quantitative accuracy evaluation method for the diagonal of the machine tool workspace and a simulation qualitative evaluation method using matlab analysis software are proposed. In addition, in order to verify the compensation effect of considering the Abbe error model, a spatial error compensation system with functions of original error analysis, high-precision modeling, diagonal error calculation and error field simulation was developed. In order to evaluate the influence of the Abbe error on the traditional spatial error model of the machine tool, we introduced an example analysis. For a three-axis machine tool, before compensation, the maximum three-axis linear error without considering the Abbe error is  $65.6\ \mu\text{m}$ ,  $24.1\ \mu\text{m}$  and  $-77.2\ \mu\text{m}$ , the maximum diagonal errors of the four bars are  $-62.5\ \mu\text{m}$ ,  $-66.7\ \mu\text{m}$ ,  $-77.2\ \mu\text{m}$  and  $-74.6\ \mu\text{m}$ , and the maximum three-axis linear errors considering the Abbe error are  $-62.4\ \mu\text{m}$ ,  $26.1\ \mu\text{m}$  and  $-63.8\ \mu\text{m}$ , four The maximum body diagonal error is  $-65.5\ \mu\text{m}$ ,  $-78.3\ \mu\text{m}$ ,  $-76.5\ \mu\text{m}$  and  $-79.7\ \mu\text{m}$  respectively. After compensation, without considering the Abbe error, the maximum three-axis linear errors are  $-15.3\ \mu\text{m}$ ,  $-12.8\ \mu\text{m}$  and  $-19.2\ \mu\text{m}$ , and the maximum diagonal errors of the four bars are  $-17.4\ \mu\text{m}$ ,  $-18.7\ \mu\text{m}$ ,  $-7.7\ \mu\text{m}$  and  $-14.3\ \mu\text{m}$  respectively. The maximum values of the three-axis linear errors considering the Abbe error are  $-16.7\ \mu\text{m}$ ,  $-14.2\ \mu\text{m}$  and  $-16.5\ \mu\text{m}$ , and the maximum values of the four-bar diagonal errors are  $9.4\ \mu\text{m}$ ,  $-6.6\ \mu\text{m}$ ,  $-4.2\ \mu\text{m}$  and  $-7.1\ \mu\text{m}$ , respectively. The experimental results show that considering the machine tool error model of Abbe error, the evaluation of machine tool accuracy is more reasonable and the compensation accuracy is higher.

## Acknowledgments

The authors would like to thank Lin Zhang, Xiangjie Wang, Chao Wang, Hua Xiang, Guangqing Tong and Dianzhang Zhao for their contributions in the writing process and also want to thank the support by the funding.

## Funding

This work was supported by 2019 Central Government Guides Local Special Funds(2019ZYD017); 2018 National Science and Technology Major Project (2018ZX04016001; 2018ZX04012001); Electromechanical Automotive Discipline Group Open Fund (2019XKQ2019001); High-end CNC machine tools and basic manufacturing equipment technology major project (2019ZX04001024).

### **Conflict of interest**

The authors declare no competing interests.

### **Data Availability**

Future The experimental data for the measuring point error used to support the findings of this study are currently embargo, while the research findings are commercialized. Request for data, 12 months after publication of this article, will be considered by the corresponding author (zjjll123456@126.com).

### **Code availability**

Not applicable.

### **Ethics approval**

Not applicable.

### **Consent to participate**

Not applicable.

### **Consent for publication**

Not applicable.

### **Contributions**

Guohua Chen: Conceptualization, methodology, formal analysis, writing. Lin Zhang: Methodology, software, investigation, writing-original draft preparation. Xiangjie Wang: Formal analysis. Chao Wang: Software, visualization. Hua Xiang: Software, methodology. Guangqing Tong : Investigation. Dianzhang Zhao: Investigation.

### **REFERENCES**

- [1] X. Zhong , H. Liu , X. Mao, "An Optimal Method for Improving Volumetric Error Compensation in Machine Tools Based on Squareness Error Identification," *International Journal of Precision Engineering and Manufacturing*. 20 (2019) 1653-1665.
- [2] Z. Zhang , L. Cai , Q. Cheng, "A geometric error budget method to improve machining accuracy reliability of multi-axis machine tools," *Journal of Intelligent Manufacturing*. 30 (2019) 495-519.
- [3] G. Cui , Y. Lu , J. Li , D. Gao , Y. Yao , Geometric error compensation software system for CNC machine tools based on NC program reconstructing, *Int. J. Adv. Manuf. Technol.* 63 (2012) 169–180 .
- [4] G. Fu , J. Fu , Y. Xu , Z. Chen , J. Lai , Accuracy enhancement of five-axis machine tool based on differential motion matrix: geometric error modeling, identification and compensation, *Int. J. Mach. Tools Manuf.* 89 (2015) 170–181 .
- [5] G. Li , Z. Wang , W. Zhu , A. Kubo , A function-oriented active form-grinding method for cylindrical gears based on error

- sensitivity, *Int. J. Adv. Manuf. Technol.* 92 (2017) 3019–3031 .
- [6] H. Schwenke , W. Knapp , H. Haitjema , A. Weckenmann , R. Schmitt , F. Delbressine , Geometric error measurement and compensation of machines—an update, *CIRP Ann.* 57 (2008) 660–675 .
- [7] H. Wang , Y. Cao , Influence of machining parameters on vibration characteristics of gear form grinding, *J. Ad. Appl. Math.* 3 (2018) 73–81.
- [8] H.-j. Xia , W.-c. Peng , X.-b. Ouyang , X.-d. Chen , S.-j. Wang , X. Chen , Identification of geometric errors of rotary axis on multi-axis machine tool based on kinematic analysis method using double ball bar, *Int. J. Mach. Tools Manuf.* 122 (2017) 161–175.
- [9] I. 230-7, Test Code for Machine Tools-Part 7: Geometric Accuracy of Axes of Rotation, 2006.
- [10] ISO1328-1-2013, Cylindrical gears—ISO system of flank tolerance classification — Part 1: Definitions and allowable values of deviations relevant to flanks of gear teeth, 2013.
- [11] J. Mayr , J. Jedrzejewski , E. Uhlmann , M. Alkan Donmez , W. Knapp , F. Härtig , K. Wendt , T. Moriwaki , P. Shore , R. Schmitt , C. Brecher , T. Würz , K. Wegener , Thermal issues in machine tools, *CIRP Ann.* 61 (2012) 771–791.
- [12] J. Wang , J. Guo , B. Zhou , J. Xiao , The detection of rotary axis of NC machine tool based on multi-station and time-sharing measurement, *Measurement.* 45 (2012) 1713–1722.
- [13] López De Lacalle LN, Lamikiz A, Ocerin O, Díez D, Maidagan E The Denavit and Hartenberg approach applied to evaluate the consequences in the tool tip position of geometrical errors in five-axis milling centres. *Int J Adv Manuf Technol.* 37(2008) 122–139.
- [14] Mehrdad V, Behrooz A Accuracy improvement of volumetric error modeling in CNC machine tools. *Int J Adv Manuf Technol.* 95 (2018) 2243–2257.
- [15] Nojedeh MV, Habibi M, Arezoo B Tool path accuracy enhancement through geometrical error compensation. *Int J Mach Tools Manuf.* 51 (2011) 471–482.
- [16] H. Liu, E. Miao, X. Zhuang, “Thermal error robust modeling method for CNC machine tools based on a split unbiased estimation algorithm,” *Precision Engineering.* 51 (2018).
- [17] Kim K. Volumetric accuracy analysis based on generalized geometric multi-axis machine tools[J]. *Mechanism and machine theory*, 1991.
- [18] G. Chen, H. Xiang, J. Chen, “A Method of Measurement and Modeling for Volumetric Errors of machine tools Based on Comprehensive Compensation,” *Revista de la Facultad de Ingeniería.* 32(2017) 332-337.
- [19] W. Zuo , W. Li , “Study on volume error model and identification method of 5-axis CNC machine tools,” *Journal of Combined Machine Tools and Automatic Machining Technology.* 2 (2019) 45-48.
- [20] Y. Zhang, H. Qin, Q. Yang, W. Li, “Error Analysis and Modeling of Grinding System of Cycloid Wheel Grinder of RV Reducer,” *Combined machine tool and automatic processing technology.* 22 (2019) 62-66.
- [21] Niels B, Jun Q, Dominiek R Design and experimental validation of an ultra-precision Abbe-compliant linear encoder-based position measurement system. *Precis Eng.* 47(2017) 197–211.

- [22] Kim DM, Lee DY, Gweon DG A new nano-accuracy AFM system for minimizing Abbe errors and the evaluation of its measuring uncertainty. *Ultramicroscopy*. 107 (2007) 322–328.
- [23] Jin T, Ji HD, Hou WM, Le YF, Shen L Measurement of straightness without Abbe error using an enhanced differential plane mirror interferometer. *Appl Opt* 56 (2017) 607–610.
- [24] Liu HW, Xiang H, Chen JH, Yang R Measurement and compensation of machine tool geometry error based on Abbe principle. *Int J Adv Manuf Technol* 98 (2018) 2769–2774.
- [25] Wang H, Li TJ, “Tolerance analysis of the volumetric error of heavy-duty machine tool based on interval uncertainty,” *International journal of advanced manufacturing technology*. 114(2021) 2185-2199.
- [26] Zhang SY, He C, Liu XJ, Xu JH, “Kinematic chain optimization design based on deformation sensitivity analysis of a five-axis machine tool,” *international journal of advanced manufacturing technology*. 21(2020) 2375-2389.
- [27] Wang HW, Ran Y, Zhang SY, Li YL, “Coupling and decoupling measurement method of complete geometric errors for multi-axis machine tools,” *Applied sciences-basel*. 10(2020) 2169-2183.